

## Tolman-Bondi collapse in scalar-tensor theories as a probe of gravitational memory

T. Harada\*

Department of Physics, Waseda University, Shinjuku, Tokyo 169-8555, Japan

C. Goymer and B. J. Carr

Astronomy Unit, Queen Mary, University of London, Mile End Road, London E1 4NS, England

(Received 25 December 2001; published 26 November 2002)

In cosmological models with a varying gravitational constant, it is not clear whether primordial black holes preserve the value of  $G$  at their formation epoch. We investigate this question by using the Tolman-Bondi model to study the evolution of a background scalar field when a black hole forms from the collapse of dust in a flat Friedmann universe. Providing the back reaction of the scalar field on the metric can be neglected, we find that the value of the scalar field at the event horizon very quickly assumes the background cosmological value. This suggests that there is very little gravitational memory.

DOI: 10.1103/PhysRevD.66.104023

PACS number(s): 04.70.Bw, 04.50.+h, 97.60.Lf, 98.80.Cq

## I. INTRODUCTION

Scalar-tensor (ST) theories of gravity provide a natural alternative to general relativity (GR). They describe gravity with not only a metric  $g_{ab}$  but also a scalar field  $\phi$ . Derivatives of  $\phi$  appear as source terms in the field equations and  $\phi$  itself satisfies a wave equation. The strength of the gravitational coupling is determined by the function  $\omega(\phi)$ , where GR is recovered in the limits  $\omega \rightarrow \infty$  and  $\omega^{-3}(d\omega/d\phi) \rightarrow 0$ .

ST theories can also be regarded as being equivalent to GR with a varying gravitational “constant”  $G$ . The most simple example of such a ST theory is Brans-Dicke theory [1], where  $\omega(\phi)$  is constant and  $G \propto \phi^{-1}$ . However, weak field experiments have shown that  $\omega > 500$  [2] and so the deviation from GR is small. For more general ST theories, where  $\omega$  is not constant, it is possible that  $\omega$  was much smaller at earlier times. So observations allow such theories to greatly deviate from GR in the early universe.

There has been a renewed interest in ST theories in recent years due to the effective low energy actions of string theory involving one or more scalar fields. These scalar fields enter the field equations in much the same way as the scalar field in ST theories [3]. Also, the increasing popularity of inflation and quintessence suggests that scalar fields might need to be incorporated into cosmological models.

The purpose of this paper is to study the effect of an evolving scalar field on the formation and evolution of a primordial black hole. In an asymptotically flat spacetime it is well known that a black hole radiates away any inhomogeneities in the scalar field until it becomes a stationary solution with constant  $\phi$  [4]. This is a consequence of the famous “no hair” theorem. However, in ST cosmological models the scalar field is evolving with time and this would modify how the black hole evolves during its lifetime.

Barrow [5] was the first to examine this problem. He considered the two extreme possibilities: scenario (A), where the scalar field evolves everywhere homogeneously in the same way as the cosmological background; and scenario (B),

where the black hole forces the scalar field to remain constant in some local region around it. The second scenario Barrow called gravitational memory because the black hole would locally preserve the value of the scalar field from when it formed. Barrow and Carr [6] studied the evolution of primordial black holes for these scenarios and found that either case results in a significant deviation from the usual GR analysis. They considered ST theories, where  $G(\phi) \propto \phi^{-1}$  as in the Brans-Dicke case. Since  $\phi$  increases with cosmological time, this implies that  $G(\phi)$  decreases, so black holes would take longer to radiate away their mass via Hawking evaporation than in the GR case. In both scenarios the black holes form when gravity is stronger, so the rate of evaporation is less, but in scenario (B) the strength never decreases and so the lifetime is even longer.

The above scenarios are the two extremes and the reality is probably somewhere in between. Two more general scenarios have been proposed [7]. In scenario (C) the scalar field evolves faster at the event horizon (EH) than at the particle horizon (PH), so  $\dot{\phi}_{EH} > \dot{\phi}_{PH}$ . Eventually the black hole must reach a stage where  $\dot{\phi}_{EH} = \dot{\phi}_{PH}$ , but this does not necessarily mean the scalar field is homogeneous since there could be some lag between the asymptotic and local increase. In scenario (D), the scalar field is evolving locally but at a slower rate than asymptotically, so  $\dot{\phi}_{EH} < \dot{\phi}_{PH}$ . There is still some gravitational memory but not in the strict sense of scenario (B). In this scenario the gradient of the scalar field is increasing but one would expect there to be some limit, due to the influx of scalar gravitational waves.

Gravitational memory for black holes which are small compared to the cosmological scale (i.e., the particle horizon) has already been investigated by Jacobson [8]. In this case, the scalar field evolution can be considered as an asymptotic perturbation to the Schwarzschild metric and the end-state of scenario (C) applies, with the lag being found to be small. This suggests that gravitational memory is virtually nonexistent. However, this approximation may not apply for primordial black holes since these can have a size comparable to the particle horizon at formation [9]. It is still not clear what would happen in this case. Therefore another way

\*Electronic address: harada@gravity.phys.waseda.ac.jp

of investigating gravitational memory, without assuming that the black hole is small, is needed.

In GR there have been several attempts to study analytic solutions which represent black holes within a cosmological background. The earliest used the Einstein-Straus solution [10], which matches a Schwarzschild interior to a Friedmann exterior, and this approach has also been used to study gravitational memory [11]. However, in most circumstances it can be shown [12] that such a matching is only possible if the scalar field is constant, which just gives the GR solution. Another method used the McVittie metric [13], but it has been shown [14] that this has a scalar curvature singularity at the event horizon.

A more successful method uses the Tolman-Bondi metric [15] to represent the collapse of dust to a black hole in an asymptotically Friedmann background. However, this only works for dust and cannot in general be applied to ST theories due to the derivatives of the scalar field appearing as source terms in the field equations. In this paper we overcome this problem by assuming that the effect of the scalar field on the spacetime is small compared to that of the matter. This means that we can use the usual Einstein field equations to generate the spacetime and then use the wave equation for the scalar field to determine its evolution. This approximation was used by Harada *et al.* [16] to calculate the scalar gravitational radiation emitted by Oppenheimer-Snyder collapse in ST theory. Jacobson also uses this approximation when calculating the effect of an evolving scalar field in Schwarzschild spacetime. We note, however, that self-consistent numerical calculations of spherical gravitational collapse in ST theory in asymptotically flat spacetime, in which the effect of the scalar field on the spacetime is fully incorporated, have been considered by previous authors [17,18].

If one makes this approximation to investigate gravitational collapse in a Tolman-Bondi spacetime, the solution is specified by two arbitrary functions: the energy and mass functions. To represent collapse in a Friedmann background, the energy function has to be negative within some radius  $r_0$  and zero outside it. This results in the eventual gravitational collapse of all the matter within  $r_0$ , while the matter outside  $r_0$  expands forever as in a flat Friedmann model. In choosing the mass function, or equivalently the density perturbation, we adopt the “compensated” model. This means that the overdense region in the center is surrounded by an underdense region outside, so that the total mass at infinity is unaffected.

We solve the field equations numerically using the characteristic method. This method was first applied to an inhomogeneous and dynamical background spacetime by Iguchi *et al.* [19]. The characteristic method integrates over null hypersurfaces with the event horizon as a boundary. This means that one never needs to calculate anything inside the black hole, thereby avoiding any numerical problems associated with singularities. The output of the code shows the spatial and temporal variation of the scalar field. The figures produced show that the initial collapse results in a large gradient in the scalar field. However, as time increases, the scalar field becomes almost homogeneous. This suggests that, within the

approximation used, gravitational memory is not possible. It remains to be seen whether the back reaction of the scalar field could alter this conclusion.

In Sec. II we describe ST theories in more detail and derive the field equations for the approximation in which the effect of the scalar field on the metric is neglected. In Sec. III we transform the Tolman-Bondi solution into null coordinates, giving the equations necessary to apply the characteristic method. In Sec. IV we specify the model giving rise to black hole formation. We present the numerical results in Sec. V and discuss their implications in Sec. VI.

## II. BASIC EQUATIONS

For scalar-tensor theories of gravity with  $G(\phi) \propto \phi^{-1}$  the field equations are

$$G_{ab} = \frac{8\pi}{\phi} T_{ab} + \frac{\omega(\phi)}{\phi^2} \left( \partial_a \phi \partial_b \phi - \frac{1}{2} g_{ab} \phi^c \phi_c \right) + \frac{1}{\phi} (\nabla_a \nabla_b \phi - g_{ab} \nabla^c \nabla_c \phi), \quad (2.1)$$

$$\nabla^c \nabla_c \phi = \frac{8\pi T - (d\omega/d\phi) \partial^c \phi \partial_c \phi}{3 + 2\omega(\phi)}, \quad (2.2)$$

where  $T_{ab}$  is the usual energy-momentum tensor,  $T$  is its trace, and we have set  $c=1$ . In Brans-Dicke theory Eq. (2.1) remains unchanged but  $d\omega/d\phi=0$  in Eq. (2.2). These equations are expressed in the Jordan frame but ST theories can also be expressed in a conformal frame known as the Einstein frame. The Einstein frame is related to the Jordan frame by the transformation

$$\bar{g}_{ab} = (G_0 \phi) g_{ab} \Rightarrow \bar{T}_{ab} = (G_0 \phi)^{-1} T_{ab}, \quad (2.3)$$

where  $G_0$  is the present value of the gravitational “constant” as measured in solar system experiments. It is called the Einstein frame because it can be expressed as GR with a scalar field. However, the Jordan frame will be used throughout this paper.

In GR the Tolman-Bondi solution is given by

$$ds^2 = -dt^2 + A^2(t, r) dr^2 + R^2(t, r) [d\theta^2 + \sin^2 \theta d\psi^2], \quad (2.4)$$

where  $r$  is the comoving radial coordinate and  $R$  is given by

$$t - t_s(r) = \sqrt{\frac{R^3}{F}} G \left( -\frac{fR}{F} \right). \quad (2.5)$$

Here  $G(y)$  is a positive function given by

$$G(y) = \begin{cases} \frac{\arcsin \sqrt{y}}{y^{3/2}} - \frac{\sqrt{1-y}}{y} \text{ or } \frac{\pi - \arcsin \sqrt{y}}{y^{3/2}} + \frac{\sqrt{1-y}}{y} & (0 < y \leq 1), \\ \frac{2}{3} & (y = 0), \\ \frac{-\operatorname{arcsinh} \sqrt{-y}}{(-y)^{3/2}} - \frac{\sqrt{1-y}}{y} & (y < 0), \end{cases} \quad (2.6)$$

$t_s(r)$  is a constant of integration, and  $F(r) = 2G_0m(r)$  with  $m(r)$  being the mass within radius  $r$ .  $A$  is given by

$$A^2(t, r) = \frac{R'(t, r)^2}{1 + f(r)}, \quad (2.7)$$

and  $R$  satisfies

$$\dot{R}^2(t, r) = \frac{F(r)}{R} + f(r). \quad (2.8)$$

The density of the dust  $\rho$  is given by

$$\rho = \frac{F'}{8\pi R^2 R'}. \quad (2.9)$$

In the above, a dot denotes  $\partial_t$  and a prime denotes  $\partial_r$ .

There are two arbitrary functions in this solution: the mass function  $m(r)$  and the energy function  $f(r)$ . Investigating collapse to a black hole just requires the appropriate choice for these functions. In this paper the energy function is chosen such that

$$f(r) < 0 \text{ for } r < r_0, \quad (2.10)$$

$$f(r) = 0 \text{ for } r > r_0, \quad (2.11)$$

for some  $r_0$ . This means that when a perturbation is applied to the background dust, all the matter interior to  $r_0$  will eventually collapse to form a black hole, while the exterior matter will expand forever as in a flat Friedmann universe [20]. The mass function  $m(r)$  is determined by putting  $R = r$  at  $t = t_s(r)$  in Eq. (2.5).

The key to this approximation is that the back reaction of the scalar field is neglected. It is assumed that the effect of the scalar field on the spacetime is small compared to that of the matter. The initial configuration used is the general relativistic one with constant  $\phi$  and for simplicity Brans-Dicke theory is used. Then, to the lowest order, the evolution of  $\phi$  is determined by the wave equation:

$$[\nabla^c \nabla_c]_{TB} \phi = \frac{8\pi}{3+2\omega} T_{TB}, \quad (2.12)$$

where  $[\nabla^c \nabla_c]_{TB}$  and  $T_{TB}$  are determined for the Tolman-Bondi metric and the general relativistic solution. Using the Tolman-Bondi metric, the wave operator is given by

$$[\nabla^c \nabla_c]_{TB} \phi = -\ddot{\phi} - \frac{(AR^2)'}{AR^2} \dot{\phi} + \frac{1}{A^2} \phi'' + \frac{1}{AR^2} \left( \frac{R^2}{A} \right)' \phi'. \quad (2.13)$$

### III. CHARACTERISTIC METHOD

The last equation needs to be rewritten in terms of a null coordinate suitable for the characteristic method. The retarded time coordinate  $u$  is introduced such that  $u = \text{constant}$  is an outgoing null geodesic. In the original coordinates the outgoing null geodesic is given by

$$\frac{dt}{dr} = A, \quad (3.1)$$

so we can write

$$\frac{u'}{\dot{u}} = -A. \quad (3.2)$$

The coordinate system is now transformed from  $(t, r)$  to  $[u(t, r), \bar{r}(r)]$  using the relations

$$du = \frac{1}{\alpha} (dt - A dr), \quad d\bar{r} = dr, \quad (3.3)$$

where

$$\alpha \equiv \frac{1}{\dot{u}}. \quad (3.4)$$

The partial derivatives are then related by

$$\partial_t = \frac{1}{\alpha} \partial_u, \quad \partial_r = -\frac{A}{\alpha} \partial_u + \partial_{\bar{r}}. \quad (3.5)$$

In this coordinate system the metric becomes

$$ds^2 = -\alpha^2 du^2 - 2\alpha A(u, \bar{r}) du d\bar{r} + R^2(u, \bar{r}) [d\theta^2 + \sin^2 \theta d\psi^2]. \quad (3.6)$$

To use the characteristic method it is necessary to introduce the derivative along the ingoing radial null geodesic. In the original coordinates the ingoing null geodesic is given by

$$\frac{dt}{dr} = -A, \quad (3.7)$$

which in the new coordinate system becomes

$$\frac{d\bar{r}}{du} = -\frac{\alpha}{2A}. \quad (3.8)$$

Therefore the derivative along the ingoing null can be obtained:

$$\frac{d}{du} = \partial_u + \frac{d\bar{r}}{du} \partial_{\bar{r}} = \frac{\alpha}{2} \left( \partial_t - \frac{1}{A} \partial_r \right). \quad (3.9)$$

The partial derivatives  $\partial_t$  and  $\partial_r$  can now be rewritten in terms of  $d/du$  and  $\partial_{\bar{r}}$ :

$$\partial_t = \frac{1}{\alpha} \frac{d}{du} + \frac{1}{2} \frac{1}{A} \partial_{\bar{r}}, \quad (3.10)$$

$$\partial_r = -\frac{A}{\alpha} \frac{d}{du} + \frac{1}{2} \partial_{\bar{r}}. \quad (3.11)$$

The wave operator then becomes

$$[\nabla^c \nabla_c] \phi = -\frac{2}{\alpha A R} \frac{d\varphi}{du} - \frac{A'}{A^3 R} \varphi + \frac{1}{AR} \left[ (A\dot{R}) \cdot - \left( \frac{R'}{A} \right)' \right] \phi, \quad (3.12)$$

where

$$\varphi \equiv \partial_{\bar{r}}(R\phi). \quad (3.13)$$

Here the dot and prime refer to the operators given in Eqs. (3.10) and (3.11), respectively. It is also necessary to obtain an equation for  $\alpha$ . This is achieved by using  $(\dot{u})' = (\dot{u}')$ , which gives

$$\partial_{\bar{r}}\alpha = \dot{A}\alpha. \quad (3.14)$$

Applying the full Tolman-Bondi solution, the basic equations that must be solved in Brans-Dicke theory are to first order

$$\begin{aligned} \frac{d\varphi}{du} &= \frac{\alpha}{2} \frac{\sqrt{1+f}}{R'} \left( \frac{f'}{2(1+f)} - \frac{R''}{R'} \right) \varphi + \frac{\alpha}{2} \frac{F}{R\sqrt{1+f}} \left( \frac{F'}{2F} \right. \\ &\quad \left. - \frac{R'}{R} \right) \phi + \frac{\alpha}{2} \frac{1}{3+2\omega} \frac{F'}{R\sqrt{1+f}}, \end{aligned} \quad (3.15)$$

$$\partial_{\bar{r}}\alpha = \pm \frac{\alpha}{2} \frac{1}{\sqrt{(1+f)\left(\frac{F}{R}+f\right)}} \left( \frac{F'}{R} - \frac{FR'}{R^2} + f' \right), \quad (3.16)$$

where the upper and lower signs correspond to an expanding and collapsing phase respectively. For numerical purposes it

is also convenient to take the parametrized form of the Tolman-Bondi solution. For  $f=0$ ,  $R$  is given by

$$R = \left( \frac{9F}{4} \right)^{1/3} [t - t_s(r)]^{2/3}. \quad (3.17)$$

For  $f>0$ , it is given by

$$R = \frac{F}{2f} (\cosh \eta - 1), \quad (3.18)$$

$$t - t_s(r) = \frac{F}{2f^{3/2}} (\sinh \eta - \eta). \quad (3.19)$$

For  $f<0$ , it is given by

$$R = \frac{F}{2(-f)} (1 - \cos \eta), \quad (3.20)$$

$$t - t_s(r) = \frac{F}{2(-f)^{3/2}} (\eta - \sin \eta). \quad (3.21)$$

Here the signs are chosen so that they correspond to the big bang universe.

#### IV. MODELS

We choose the background primordial black hole model so that the following conditions are satisfied. (1) The big bang occurs at the same time everywhere, i.e.,  $t_s(r)=0$  (constant). (2) The model is asymptotically flat Friedmann and compensated (i.e., the overdense region in the center is surrounded by an underdense region outside in such a way that the total mass at infinity is unaffected). (3) The model is free of shell-focusing or shell-crossing naked singularities, at least within the calculated region. (4) The central region is bound, while the asymptotic region is marginally bound. (5) At the initial time  $t=t_0$ , the condition  $R'>0$  is satisfied everywhere.

In order to satisfy the above conditions, we set  $t=t_0$  and choose the energy function  $f(r)$  to have the form

$$f(r) = \begin{cases} -\left(\frac{r}{r_c}\right)^2 & \text{for } r < r_w, \\ -\left(\frac{r}{r_c}\right)^2 \exp\left(-\left(\frac{r-r_w}{r_w}\right)^4\right) & \text{for } r \geq r_w, \end{cases} \quad (4.1)$$

where  $r_c$  gives the curvature radius in the central closed Friedmann region and  $r_w$  gives the scale of the overdense region. Equation (4.1) means that the central region  $r < r_w$  is described by the exact closed Friedmann solution, which ensures that there is no shell-focusing naked singularity. More general situations in which shell-focusing is avoided have been discussed elsewhere [21]. The code continually monitors for shell-crossing to check that this never happens within the calculated region. We then determine  $F(r)$  so that  $r$  coincides with  $R$  at the  $t=t_0$  spacelike hypersurface.

TABLE I. Parameters for models.

Models	$f$	$H_0 r_c$	$H_0 r_w$	Initial data
A	(4.1)	2	1.25	$\phi_c$
B	(4.1)	2	1	$\phi_c$
C	(4.1)	3	1.25	$\phi_c$
D	(4.1)	2	1.25	$\phi_+$
E	(4.1)	2	1.25	$\phi_-$
F	(4.2)	2	3	$\phi_c$

The choice of the function  $f(r)$  requires some justification since it is nowhere exactly zero in the calculated region, so strictly speaking the entire region would eventually collapse to a black hole if one waited long enough. In practice, this does not matter because our calculated region is so large that the value of  $f$  is effectively identical to 0 for  $r \gtrsim 5 r_w$  (i.e., at the outer boundary). Since the region is finite, we can therefore always make the matching to the Einstein-de Sitter universe *outside* the calculated region. It would be easy in principle to perform the calculations for a situation in which the matching occurs *within* the calculated region (i.e., with  $f = 0$  exactly at the edge of the region). It is clear that this would make no qualitative difference to our conclusions but, to confirm this, we also adopt the choice

$$f(r) = \begin{cases} -\left(\frac{r}{r_c}\right)^2 \left[1 - \left(\frac{r}{r_w}\right)^4\right]^4 & \text{for } r < r_w, \\ 0 & \text{for } r \geq r_w, \end{cases} \quad (4.2)$$

in which the compensation is satisfied explicitly within the calculated region.

Before integrating, we have to fix the initial data for  $\phi$ . One can take this to be the homogeneous cosmological solution given by

$$\phi_c = \phi_0 \left( 1 + \frac{1}{3+2\omega} \frac{4}{3} \ln \frac{t}{t_0} \right). \quad (4.3)$$

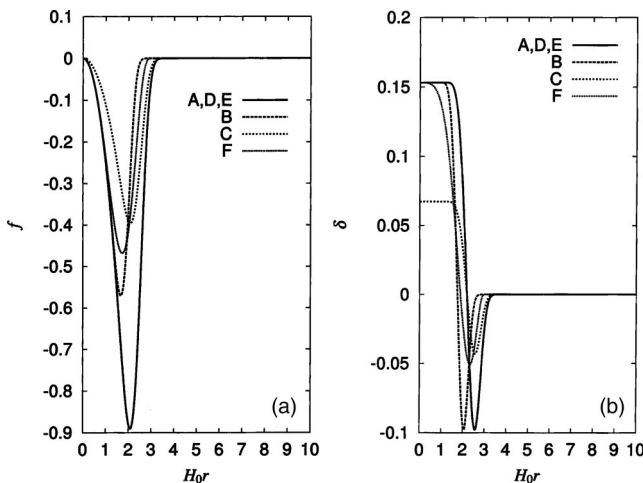
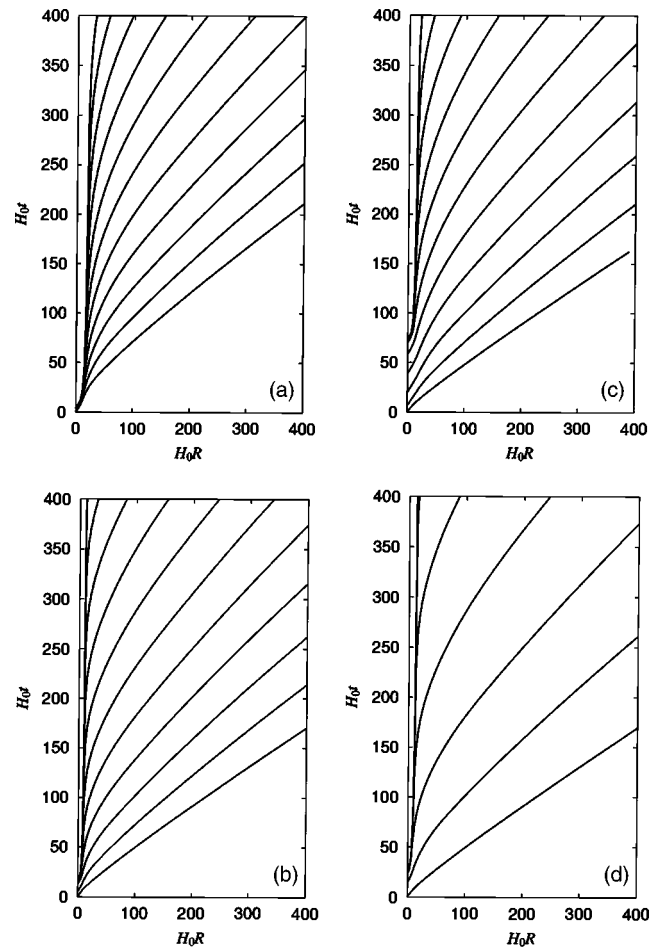
FIG. 1. (a) Energy function  $f$  and (b) initial density perturbation  $\delta$  are plotted for models A–F.

FIG. 2. Trajectories of outgoing null rays are plotted (a) for models A, D, E, (b) for model B, (c) for model C, and (d) for model F.

We then set the initial null hypersurface as the null cone whose vertex is at  $(t, r) = (t_0, 0)$  and regard the cosmological solution as the initial data on this hypersurface. Although the value of the scalar field at the cosmological particle horizon must be given by this solution, the value in the perturbed region and the surrounding region may be different from this. To examine the sensitivity of the results to this alteration, we consider another form of the initial data which is different from the cosmological solution in the region  $t \leq (1-10) \times t_0$ . We now choose

$$\phi_{\pm} = \phi_c \left[ 1 \pm \exp \left[ -\left( \frac{t}{5t_0} \right)^2 \right] \right], \quad (4.4)$$

so that we have an ingoing wave in the perturbed region, and examine the evolution of the scalar field thereafter. The numerical code has been checked by the following nontrivial test calculation. In the flat Friedmann universe, the code must reproduce the cosmological evolution Eq. (4.3) from the initial data. There is agreement to within 0.05% accuracy.

## V. RESULTS

We denote the Hubble parameter in the Friedmann background (far from the perturbed region) as  $H_0$  at  $t = t_0$ . Recall

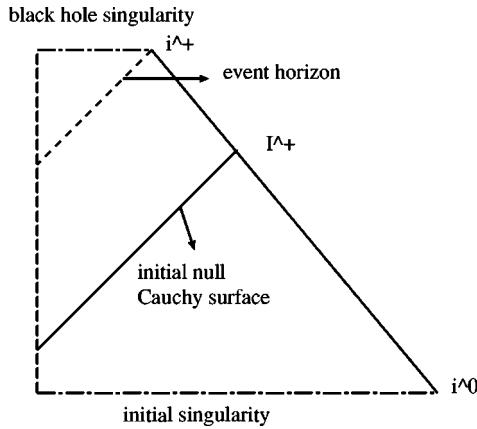


FIG. 3. Penrose diagram of a primordial black hole in a flat Friedmann universe. Also depicted is the null Cauchy surface on which the initial conditions are set for the numerical calculations.

that  $r_c$  gives the amplitude of the density perturbation, while  $r_w$  gives the size of the perturbed region. For superhorizon scale perturbations, we cannot set the density perturbation to be very large else the overdense region closes up on itself and becomes disconnected from the rest of the universe [9]. Actually, the requirement  $R'>0$  imposes an even stronger condition since it implies  $r_w \leq r_c$ . We have set the Brans-Dicke parameter to be  $\omega=5$ . If  $r_c$  is much increased, then the amplitude of the overdensity is much decreased and the resulting black hole becomes very small compared with the horizon scale at the formation time. If  $r_c$  is much decreased, the overdense region becomes a separate closed universe. Models and parameters are summarized in Table I. The difference between models A, B, C, and F is in the choice of the background perturbation. The difference between models A, D, and E is in the choice of the initial condition for the scalar field. A change of  $\omega$  only scales the variation of the scalar field from  $\phi_0$ , as indicated by Eq. (4.3).

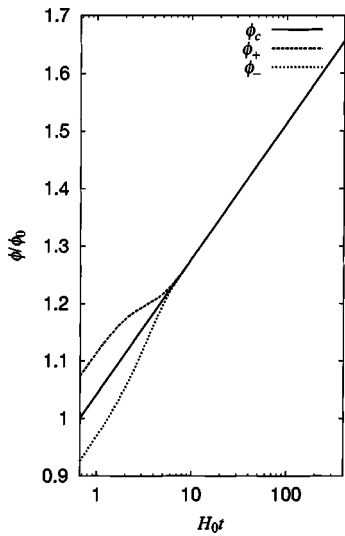


FIG. 4. Initial null Cauchy data sets for the scalar field:  $\phi_c$  for models A, B, C, and F;  $\phi_+$  for model D; and  $\phi_-$  for model E. For clarity, the abscissa is plotted logarithmically.

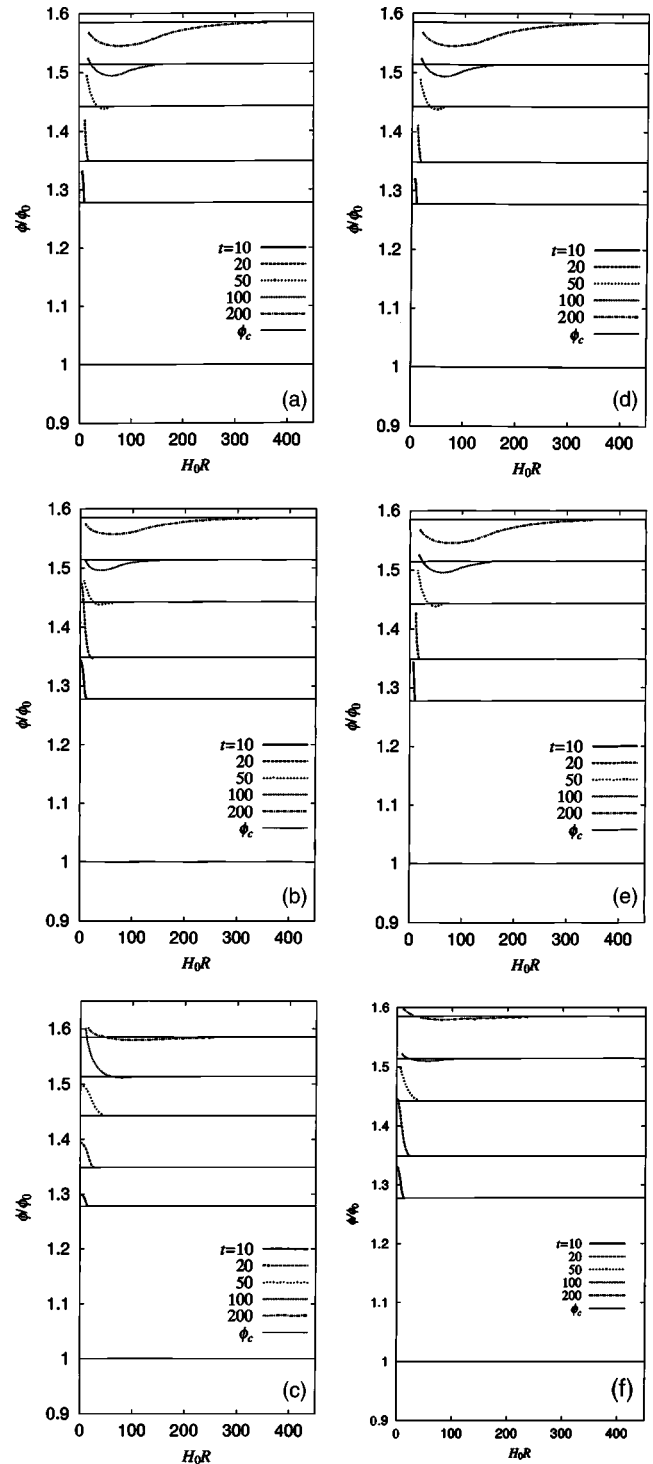


FIG. 5. Configuration of the scalar field at each moment  $t = \text{const}$  is plotted for models (a) A, (b) B, (c) C, (d) D, (e) E, and (f) F. For comparison, the cosmological value  $\phi_c$  at each moment is also plotted as a horizontal line.

In Fig. 1, the energy function  $f(r)$  and the initial density perturbation

$$\delta(t_0, r) \equiv \frac{\rho(t_0, r) - \rho(t_0, \infty)}{\rho(t_0, \infty)} \quad (5.1)$$

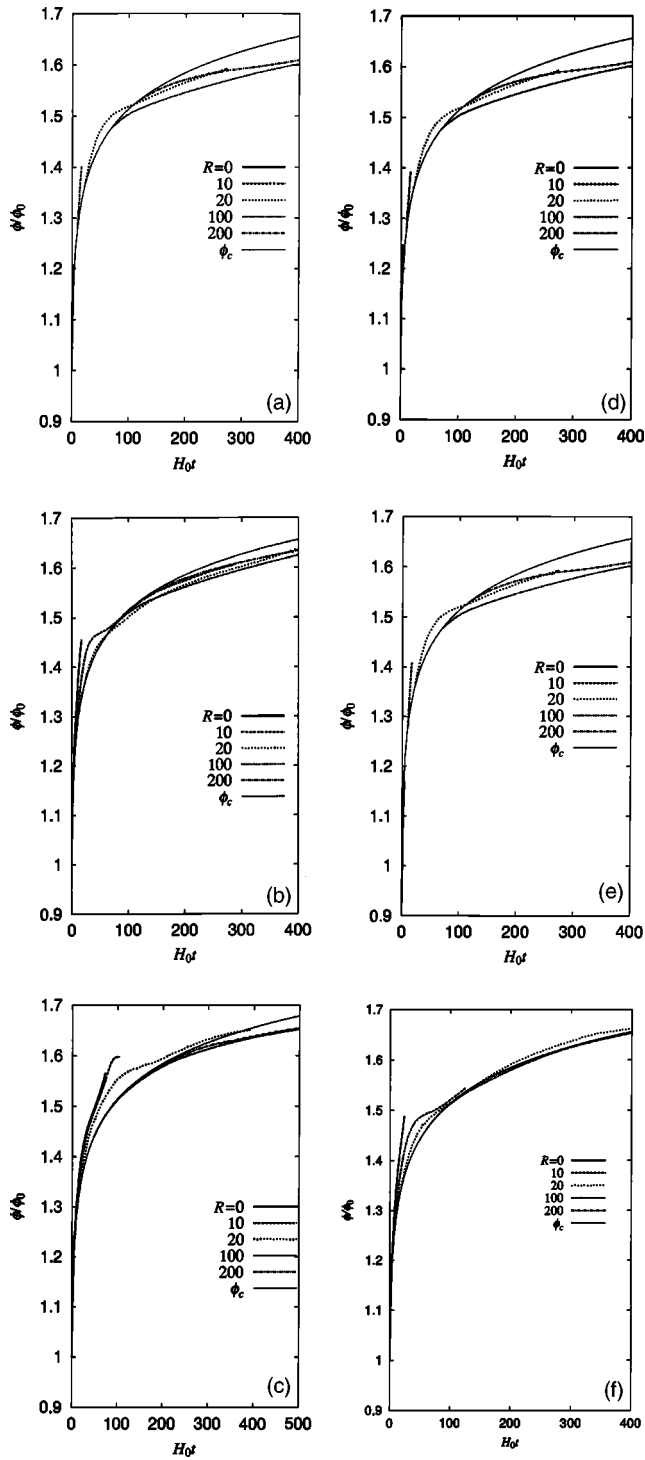


FIG. 6. Time variation of the scalar field along the world-lines of constant  $R$  is plotted for models (a) A, (b) B, (c) C, (d) D, (e) E, and (f) F. For comparison, the cosmological evolution  $\phi_c$  is also plotted.

are plotted. The trajectories of outgoing null geodesics are plotted in Fig. 2. It is seen that a nearly horizon-scale black hole is formed for model A, while the black hole is smaller than the horizon scale for models B, C, and F. This is because the size of the black hole is always roughly  $20H_0^{-1}$ , whereas the time at which it forms is about  $20H_0^{-1}$  in model

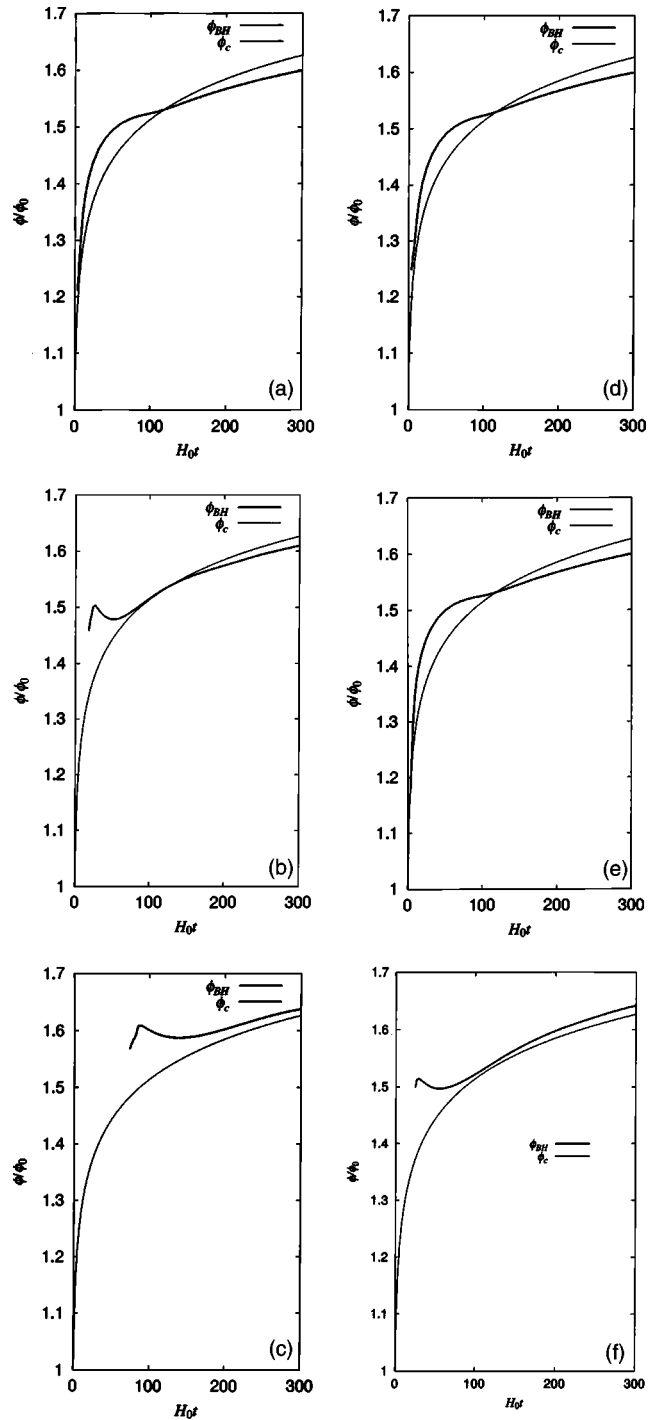


FIG. 7. Time evolution of the scalar field on the event horizon is plotted for models (a) A, (b) B, (c) C, (d) D, (e) E, and (f) F. For comparison, the cosmological evolution  $\phi_c$  is also plotted.

A and closer to  $100H_0^{-1}$  in the other cases. The initial data for the scalar field are set on the initial null Cauchy surface (see Fig. 3). We prepare three sets of initial data,  $\phi_c$ ,  $\phi_+$  and  $\phi_-$ , and these are plotted in Fig. 4. We have investigated all the models listed in Table I and the results are seen in Figs. 5–7. In Fig. 5, the profile of the scalar field is plotted for constant  $t$ . In Fig. 6, it is plotted for constant  $R$ . The reason why some of the curves come to an abrupt end *below* some

value of  $R$  is that the event horizon has formed near the center and we did not calculate the evolution of the scalar field inside the event horizon. The reason why some of them come to an abrupt end *above* some value of  $R$  is due to the finiteness of the region in which the numerical calculation is done.

We note that collapse ensures that the scalar field is initially concentrated in the central regions and this means that it rises above the asymptotic cosmological value everywhere. However, this central concentration tends to fall due to the underdensity surrounding the black hole. This effect, coupled with the increase of the cosmological value, means that the scalar field necessarily falls below the cosmological value at sufficiently large values of  $R$ , at least for the models under consideration. Eventually it may do so at every plotted value of  $R$ . Strictly speaking, the issue of gravitational memory is concerned with the process whereby the scalar field is *raised* to the cosmological value once it has fallen below it rather than with the process whereby it initially *falls* to the cosmological value.

Generally, the configuration of the scalar field tends to spatial homogeneity with increasing time and the value of the scalar field around the black hole follows the cosmological evolution of the scalar field at each moment. To see this more clearly, we identify the value of the scalar field on the latest null ray within the calculation as the value on the black hole event horizon,  $\phi_{\text{BH}}$ , because the null ray is very close to the event horizon for each model (at least for  $H_0 t \lesssim 300$ , see Fig. 2). Both  $\phi_c$  and  $\phi_{\text{BH}}$  are plotted in Fig. 7. The end of the curve  $\phi_{\text{BH}}$  corresponds to the formation time of the event horizon. We can see that  $\phi_{\text{BH}}$  follows the evolution of  $\phi_c$ . There is a small deviation of  $\phi_{\text{BH}}$  from  $\phi_c$  but this can be explained by the central overdensity and the surrounding underdensity. For  $H_0 t \lesssim 100$ , the event horizon runs through the overdense region and hence the scalar field tends to be amplified compared with  $\phi_c$ . Thereafter the event horizon runs through the underdense region and so the scalar field tends to be reduced compared with  $\phi_c$ . The overall evolution of  $\phi_{\text{BH}}$  is well described by  $\phi_c$ .

Although there are minor differences among the models, we can conclude that the configuration of the scalar field is nearly spatially homogeneous and well described by the cosmological solution  $\phi_c$ , at least for around ten initial Hubble times after the formation of the event horizon.

## VI. SUMMARY

We have calculated the evolution of the Brans-Dicke scalar field in the presence of a primordial black hole formed in a flat Friedmann background. We have found that the value of the scalar field at the event horizon almost always maintains the cosmological value. This suggests that primordial black holes “forget” the value of the gravitational constant at their formation epoch. In this sense, we confirm the result of Jacobsen [8], although he never carried out an explicit evolutionary calculation. While it is possible that some choices of the function  $f(r)$  might lead to a different conclusion, we would claim that our conclusion must at least hold in compensated models. For we have tried many sets of parameters, corresponding to models which describe a wide variety of physical situations, and this always seems to be the case. However, it is not clear from our analysis what would happen for noncompensated models and we have also avoided models with shell-crossing singularities, so we do not claim that our result is completely general.

It should also be stressed that this result has only been demonstrated for a dust universe in which the scalar field does not appreciably affect the background curvature and it remains to be seen whether the same conclusion applies when this assumption is dropped. As can be seen from Figs. 5 and 6, both the radial gradient and the time derivative of  $\phi$  are large at early times and both of these act as source terms in the field equations. However, as long as  $\omega$  is large, this is unlikely to stop the scalar field becoming homogeneous eventually, since it is clear that both the radial gradient and time derivative become small well after the initial collapse. Neglecting the back reaction should therefore be a reasonable assumption in this situation, so gravitational memory seems unlikely. However, this conclusion might not apply for  $\omega \approx 1$ .

## ACKNOWLEDGMENTS

We would like to thank T. Nakamura for helpful discussion. T.H. is supported by the Grant-in-Aid (No. 05540) from the Japanese Ministry of Education, Culture, Sports, Science and Technology. C.G. is supported by the UK Particle Physics & Astronomy Research Council.

---

[1] C. Brans and R.H. Dicke, Phys. Rev. **124**, 925 (1961).  
 [2] C.M. Will, *Theory and Experiment in Gravitational Physics* (Cambridge University Press, Cambridge, England, 1993).  
 [3] C.G. Callan *et al.*, Nucl. Phys. **B262**, 597 (1985).  
 [4] S.W. Hawking, Commun. Math. Phys. **25**, 167 (1972).  
 [5] J.D. Barrow, Phys. Rev. D **46**, R3227 (1992).  
 [6] J.D. Barrow and B.J. Carr, Phys. Rev. D **54**, 3920 (1996).  
 [7] C. Goymer and B.J. Carr (unpublished); B.J. Carr and C. Goymer, Prog. Theor. Phys. **136**, 321 (1999).  
 [8] T. Jacobson, Phys. Rev. Lett. **83**, 2699 (1999).  
 [9] B.J. Carr and S.W. Hawking, Mon. Not. R. Astron. Soc. **168**, 399 (1974).  
 [10] A.E. Einstein and E.G. Straus, Rev. Mod. Phys. **17**, 120 (1945).  
 [11] N. Sakai and J.D. Barrow, Class. Quantum Grav. **18**, 4717 (2001).  
 [12] A. Whinnett, Ph.D. thesis, 2000.  
 [13] G.C. McVittie, Mon. Not. R. Astron. Soc. **93**, 325 (1933).  
 [14] B.C. Nolan, Class. Quantum Grav. **16**, 1227 (1999).  
 [15] R.C. Tolman, Proc. Natl. Acad. Sci. U.S.A. **20**, 169 (1934); H. Bondi, Mon. Not. R. Astron. Soc. **107**, 410 (1947).  
 [16] T. Harada, T. Chiba, K. Nakao, and T. Nakamura, Phys. Rev. D **55**, 2024 (1997).

- [17] M. Shibata, K. Nakao, and T. Nakamura, Phys. Rev. D **50**, 7304 (1994).
- [18] M.A. Scheel, S.L. Shapiro, and S.A. Teukolsky, Phys. Rev. D **51**, 4208 (1995).
- [19] H. Iguchi, K. Nakao, and T. Harada, Phys. Rev. D **57**, 7262 (1998); H. Iguchi, T. Harada, and K. Nakao, Prog. Theor. Phys. **101**, 1235 (1999); **103**, 53 (2000).
- [20] M. Demiański and J.P. Lasota, Nature (London) **241**, 53 (1973).
- [21] P.S. Joshi, *Global Aspects in Gravitation and Cosmology* (Oxford University Press, New York, 1993).